

ARTICLE

Influence of Chemical Effect on the K_{β}/K_{α} Intensity Ratios and K_{β} Energy Shift of Co, Ni, Cu, and Zn ComplexesG. Apaydın^a, V. Aylıkçı^{a*}, Z. Bıyıklıoğlu^b, E. Tıraşoğlu^a, H. Kantekin^b*a. Department of Physics, Faculty of Arts and Sciences, Karadeniz Technical University, Trabzon 61080, Turkey**b. Department of Chemistry, Faculty of Arts and Sciences, Karadeniz Technical University, Trabzon 61080, Turkey*

(Dated: Received on March 10, 2008; Accepted on June 16, 2008)

Chemical effects on the K_{β}/K_{α} intensity ratios and ΔE energy differences for Co, Ni, Cu, and Zn complexes were investigated. The samples were excited by 59.5 keV γ -rays from a ^{241}Am annular radioactive source. K X-rays emitted by samples were counted by an Ultra-LEGe detector with a resolution of 150 eV at 5.9 keV. We observed the effects of different ligands on the K_{β}/K_{α} intensity ratios and ΔE energy differences for Co, Ni, Cu, and Zn complexes. We tried to investigate chemical effects on central atoms using the behaviors of different ligands in these complexes. The experimental values of K_{β}/K_{α} were compared with the theoretical and other experimental values of pure Co, Ni, Cu, and Zn.

Key words: Chemical effect, K intensity ratio, ΔE energy difference, Ultra-LEGe detector, ^{241}Am annular radioactive source

I. INTRODUCTION

X-ray emission spectra are known to be influenced by the chemical combination of X-ray emitting atoms with different ligands. The effects of the chemical structure are not large and a theoretical interpretation of these effects has not been established completely. Therefore, chemical effects have rarely been utilized in the characterization of materials. Moreover, the process of particle size effects, vacancy production, data analysis procedures to acquire the areas under peaks, detector efficiency, and self-absorption in the specimen have to be well controlled. If not, the measured intensity ratios can be erratic because of the effect of these conditions. The chemical effects on K shell fluorescence parameters of 3d transition elements and their compounds have been generally investigated and interpreted by a number of researchers using oxidation numbers, valence band structure, chemical bonding type, and symmetry. It is also well known that X-ray spectra depend on the chemical surroundings of the atom. Several studies concerned with chemical effect on the K_{β}/K_{α} intensity ratios of 3d transition elements and their chemical compounds were conducted [1-7]. Chemical effects on the K_{β}/K_{α} intensity ratio and K energy shift of Cr compounds were investigated with 2.5 MeV protons [8]. Nickel K_{α} fluorescence spectra were measured for 32 nickel compounds and chemical effects of the spectra were evaluated and compared for High-spin divalent compounds, metals and semiconductors, square-planar

low-spin divalent complexes, and trivalent compounds [9]. Some researchers investigated the chemical effects on the satellite lines of sulfur K_{β} emission spectra in several sulfur compounds [10]. K_{α} X-ray satellite spectra of sulfur compounds were measured and the effect of chemical environment was interpreted with regard to the lifetimes of L-shell vacancies and the transitions between the ligand and central atom [11]. The nickel K_{α} spectra of oxides, halides, complex compounds, and metal were measured and the peak shifts and line width varies due to the changes in chemical states were reported [12]. Similarly, chemical shifts and main absorption peak in eight manganese compounds were reported and the molecular orbital theory was employed to interpret the shifts observed with the change in the oxidation state and in the ligands of the manganese atom. As a result, it was shown that the most important factor causing the chemical shifts was the valency [13]. Chemical effects on the K_{β}/K_{α} and L_i/L_{α} ($i=\alpha, \beta, l, \eta$) X-ray intensity ratios, L shell cross-sections and fluorescence parameters were investigated by our group [14-17].

In the present work, we measured the K_{β}/K_{α} intensity ratios and ΔE energy differences of Co, Ni, Cu, and Zn complexes, and investigated the effect of chemical environment and chemical structures using the nature of ligands and relationship between the central atoms and ligands in chemical complexes because these parameters depend on the physical and chemical environments of the elements in the sample.

II. EXPERIMENTS

The studied complexes are illustrated in Fig.1. Co, Ni, Cu, Zn, 2B-Co [18], 2B-Ni [18], Cyc-Ni-Pc [19], Cyc-Zn-Pc [19], 2B-Co-Pc [20], 2B-Ni-Pc [20], 2B-Cu-Pc [20], 2B-Zn-Pc [20], Py-Co-Pc [21], Py-Ni-Pc [21], Py-

* Author to whom correspondence should be addressed. E-mail: v_aylikci@ktu.edu.tr; Tel: +90-462-377254; FAX: +90-462-3253195

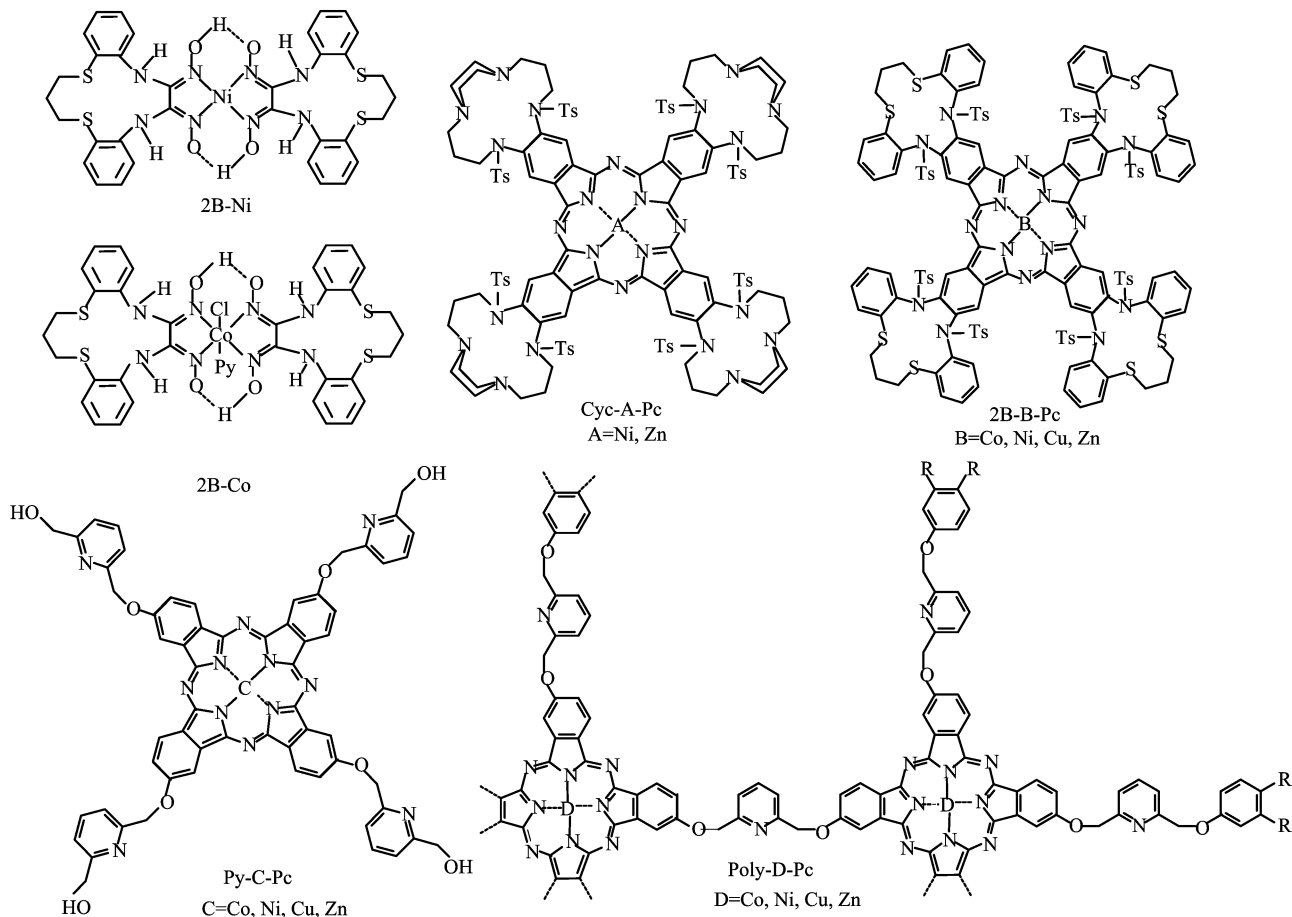


FIG. 1 The structural formula of studied complexes.

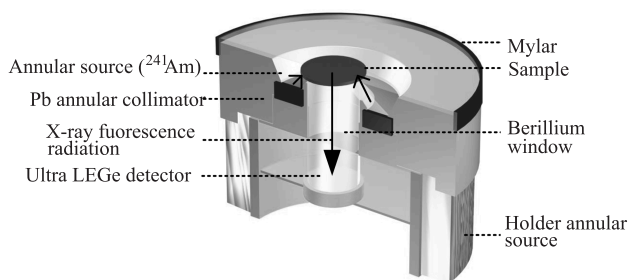


FIG. 2 Geometry of the experimental set-up.

Cu-Pc [21], Py-Zn-Pc [21], Poly-Co-Pc [22], Poly-Ni-Pc [22], Poly-Cu-Pc [22], and Poly-Zn-Pc [22] complexes were prepared according to published procedures. Pure samples were obtained commercially and the purity of the materials was >99%. Powder samples were sieved using 400 mesh and the particle sizes were so sufficiently small that there was no significant correction to the data. After that, these samples were prepared by supporting on a mylar film of 0.55-1.45 mg/cm² thickness.

The geometry of the experimental set-up is shown in Fig.2 and the live time was selected as 5000 s for each

sample. In order to reduce the statistical error in the experimental measurements, the measurements were repeated three times on the same target and the spectra were analysed by using Origin software program. In this experimental set-up, 59.5 keV gamma photons emitted by an annular 50 mCi ^{241}Am radioactive source were used. The fluorescence K X-ray from the sample was detected by a collimated Ultra-LEGe detector having a thickness of 5 mm and an energy resolution of 150 eV at 5.96 keV. The output from the preamplifier, with a pulse pile-up rejection capability, was fed to a multi-channel analyzer interfaced with a personal computer provided with suitable software for data acquisition and peak analysis. Spectra were analyzed using the Nucleus program (Tennelec PCA II).

In the present study, Figure 3 shows the spectra of K X-rays for Zn complexes. The studied complexes were listed in Table I with the symmetries, hybridizations, and oxidation states.

The experimental K-shell X-ray intensity ratios K_{β}/K_{α} were evaluated using the equation

$$\frac{I_{K_{\beta}}}{I_{K_{\alpha}}} = \frac{N_{K_{\beta}} \beta_{K_{\alpha}} \varepsilon_{K_{\alpha}}}{N_{K_{\alpha}} \beta_{K_{\beta}} \varepsilon_{K_{\beta}}} \quad (1)$$

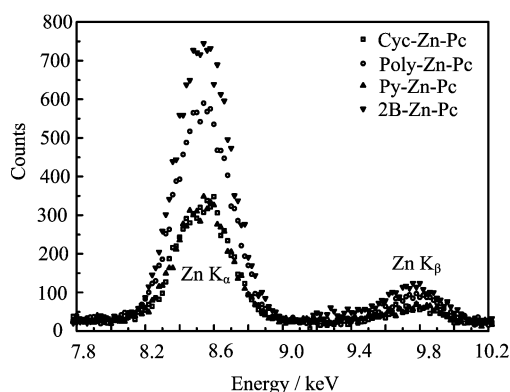


FIG. 3 Typical K X-ray spectrum for Zn complexes.

TABLE I The symmetries, hybridizations, and oxidation states for studied complexes.

Complexes	Symmetry	Hybridization	Oxidation state
Co			0
2B-Co-Pc	D _{4h}	sp ³	+2
2B-Co	O _h	d ² sp ³	+3
Poly-Co-Pc	D _{4h}	sp ³	+2
Py-Co-Pc	D _{4h}	sp ³	+2
Ni			0
2B-Ni-Pc	D _{4h}	dsp ²	+2
2B-Ni	D _{4h}	dsp ²	+2
Cyc-Ni-Pc	D _{4h}	dsp ²	+2
Poly-Ni-Pc	D _{4h}	dsp ²	+2
Py-Ni-Pc	D _{4h}	dsp ²	+2
Cu			0
2B-Cu-Pc	D _{4h}	sp ³	+1
Poly-Cu-Pc	D _{4h}	sp ³	+1
Py-Cu-Pc	D _{4h}	sp ³	+1
Zn			0
2B-Zn-Pc	D _{4h}	dsp ²	+2
Cyc-Zn-Pc	D _{4h}	dsp ²	+2
Poly-Zn-Pc	D _{4h}	dsp ²	+2
Py-Zn-Pc	D _{4h}	dsp ²	+2

where $N_{K_{\beta}}/N_{K_{\alpha}}$ represents the ratio of the counting rates under the K_{β} and K_{α} peak, $\beta_{K_{\alpha}}/\beta_{K_{\beta}}$ is the ratio of self-absorption correction factors of the target that accounts for the absorption of incident photons and emitted K X-ray photons, and $\varepsilon_{K_{\alpha}}/\varepsilon_{K_{\beta}}$ is the ratio of the detector efficiency values for K_{α} and K_{β} X-rays, respectively.

The experimental energy difference ΔE between the K_{β} and K_{α} line was evaluated using the following equation

$$\Delta E = E(K_{\beta}) - E(K_{\alpha}) \quad (2)$$

The ΔE energy differences are given in the first column of Table II. In order to reduce the statistical errors,

the positions of K_{α} and K_{β} lines for each sample were determined using the origin software program. The self absorption correction was calculated using the equation

$$\beta = \frac{1 - \exp\{[-(\mu_{\text{inc}} \csc \theta_1 + \mu_{\text{emt}} \csc \theta_2)m_i]\}}{(\mu_{\text{inc}} \csc \theta_1 + \mu_{\text{emt}} \csc \theta_2)m_i} \quad (3)$$

where μ_{inc} and μ_{emt} are the mass attenuation coefficients (cm^2/gr) of incident photons and emitted characteristic X-rays respectively [23]; the angles of incident photons and emitted X-rays with respect to the surface of the samples θ_1 and θ_2 , were equal to 45° and 90° in the present experimental set-up respectively. The product $I_0 G \varepsilon$, containing the terms related to the incident photon flux, geometrical factor and absolute efficiency of the X-ray detector, was determined by collecting the K_{α} and K_{β} X-ray spectra of samples of Cr, Fe, Zn, As, Se, Sr, Zr, Mo, Ru, and Cd in the same geometry using the equation

$$I_0 G \varepsilon_{K_i} = \frac{N_{K_i}}{\sigma_{K_i} \beta_{K_i} m_i} \quad (4)$$

where N_{K_i} is the measured intensity (area under the photopeak) corresponding to the K_i group of X-rays, I_0 is the intensity of the incident radiation, G is a geometrical factor, ε_{K_i} is the detection efficiency for the K_i group of X-rays, β_{K_i} is the self-absorption correction factor for the target material, which accounts for the absorption in the target of the incident photons and the emitted characteristic X-rays.

Theoretical values of σ_{K_i} X-ray production cross-sections were calculated using the equation

$$\sigma_{K_i} = \sigma_K(E) \omega_K f_{K_i} \quad (5)$$

where $\sigma_K(E)$ is the K-shell photoionization cross-section of the given element for the excitation energy E [24], ω_K is the K-shell fluorescence yield [25], and f_{K_i} is the emission rate of the fractional X-ray for K_{α} and K_{β} X-rays [26]. The factor $I_0 G \varepsilon_{K_i}$ was fitted as a function of energy using the equations

$$I_0 G \varepsilon_{K_i} = A_0 + A_1 E_x + A_2 E_x^2 + A_3 E_x^3 \quad (6)$$

$$I_0 G \varepsilon_{K_i} = B_0 + B_1 E_x + B_2 E_x^2 \quad (7)$$

where E_x is the K_{α} and K_{β} X-ray energy and A_0 , A_1 , A_2 , A_3 , B_0 , B_1 , and B_2 are constants evaluated from a fitting polynomial. The variation of the factor $I_0 G \varepsilon_{K_i}$ as a function of the mean K X-ray energy is shown in Fig.4.

III. RESULTS AND DISCUSSION

The measured values of K_{β}/K_{α} intensity ratios and ΔE energy differences of Co, Ni, Cu, and Zn complexes excited 59.5 keV energy are given in Table II.

The results of the measurements shown in Table II indicate that K_{β}/K_{α} intensity ratios and ΔE energy

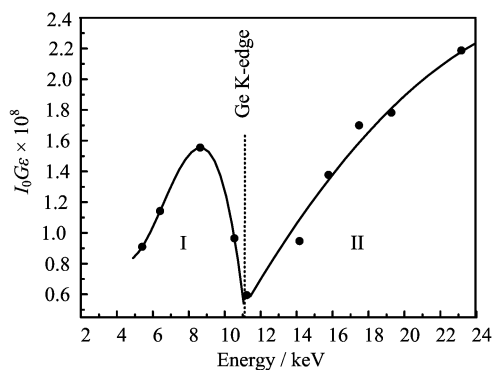


FIG. 4 The variation of the factor $I_0 G \varepsilon$ as a function of the mean K X-ray energy.

TABLE II ΔE differences and K_β/K_α intensity ratios.

Complexes	$\Delta E/eV$	K_β/K_α intensity ratios		
		Experimental	Ref.[27]	Ref.[28]
Co	694.4	0.1227	0.1218	0.1219
2B-Co-Pc	716.4	0.1261		
2B-Co	692.1	0.1669		
Poly-Co-Pc	698.1	0.1273		
Py-Co-Pc	708.6	0.1015		
Ni	778.5	0.1122	0.1227	0.1221
2B-Ni-Pc	784.8	0.0976		
2B-Ni	797.7	0.1050		
Cyc-Ni-Pc	759.4	0.0710		
Poly-Ni-Pc	865.4	0.1000		
Py-Ni-Pc	767.9	0.0902		
Cu	837.3	0.1314	0.1216	0.1208
2B-Cu-Pc	863.2	0.0989		
Poly-Cu-Pc	870.9	0.1151		
Py-Cu-Pc	869.6	0.1090		
Zn	938.9	0.1197	0.1241	0.1233
2B-Zn-Pc	922.6	0.1365		
Cyc-Zn-Pc	935.4	0.0905		
Poly-Zn-Pc	950.6	0.1130		
Py-Zn-Pc	940.9	0.0858		

differences are affected by the chemical environment of the emitting atom. The interaction between the central transition metal and ligands comes into existence in valance state and outermost 3d and 4s electrons in the close lying M_4 , M_5 , and N_1 subshells. These electrons determine the chemical properties of Co, Ni, Cu, and Zn. The intensity K_β group comes from the 3p electrons and the intensity K_α group comes from 2p electrons. Therefore, the K_β group feels the chemical effect of ligands more than the K_α group. It is well known that orbital energy levels, such as L, M, N, O, and P shells, are close to each other with increasing quantum number n . Therefore, outer energy levels are sensitive to the chemical environment with this effect

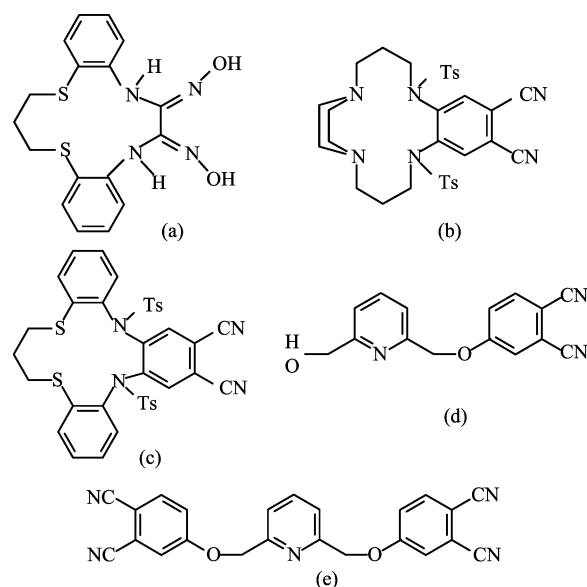


FIG. 5 The structural formula of ligand groups. (a) (6Z,7Z)-15,16-dihydro-14H-dibenzo[b,h][1,10,4,7]dithiadiazacyclotridecine-6,7(5H,8H)-dione-dioxime. (b) 1,12-Bis[(4-methyl)sulfonyl]-1,2,3,4,6,7,9,10,11,12-decahydro-5,8-ethano-1,5,8,12-benzotetraazacyclotetradecine-14,15-dicarbonitrile. (c) 5,19-Bis[(4-methyl)sulfonyl]-5,12,13,19-tetrahydro-11H-tribenzo[b,e,h][1,10,4,7]dithia-diazacyclotridecine-2,3-dicarbonitrile. (d) 4-[6-(hydroxymethyl)pyridin-2-yl]methoxy phthalonitrile. (e) 4,4'-[pyridine-2,6-diylbis(methyleneoxy)]diphthalonitrile.

and they are strongly influenced by ligands in terms of crystal field theory. In the bond formation, the valance state of the atom has an important effect on the related parameters of the spectrum such as relative intensity, Auger effect, and peak position. In the chemical compounds, some valance charge is removed (or transferred) from the atom. Consequently, the electronic screening is reduced and binding energies of the outer shells are changed. Thus, binding energies of outer shell electrons are affected by the changed valance charge.

In this study, there are four ligand groups binding the central Co, Ni, Cu, and Zn atoms and these groups are shown in Fig.5. When inductive effect and conjugation are taken into consideration in these kinds of complexes, conjugation increases because of the π bonds in the metal-ligand center. Therefore, electron delocalization on the center ring increases and this increase changes the metal-ligand interaction (increase or decrease). In addition to this, after the third degree of adjacent, the inductive effect decreases ($-I$) and this effect weakens according to the conjugation. (In the first group, the $-I$ effect of O atoms increases because of the O-N bonding).

In the first ligand group, conjugation is weaker and the inductive effect is stronger than the other ligand groups according to the centers binding the second, third, and fourth ligand groups. The oxygen atom is first degree adjacent to the nitrogen atom; hence, the

electron density on the nitrogen atom decreases according to the $-I$ effect and the coordination bonding of N-(central atom) weakens.

In the second, third, and fourth ligand groups, these groups substituted to the center ring of metallophthalocyanines create an inductive effect on the center ring and this effect is fairly weak according to the strong conjugation of π electron of ring. The strong conjugation of π electron changes the metal-ligand interaction in the metal-free phthalocyanines and the metallophthalocyanines (18 π electrons conjugate on the center ring).

The chemical effect on K_{β}/K_{α} intensity ratios and ΔE energy differences depends on valence states, coordination numbers, bond structures, nature of ligands, binding energies, crystal structures, interatomic distances and charge transfer effects. In this study, it is possible to say that the most important factors causing the changes in the K_{β}/K_{α} intensity ratios and ΔE energy differences are the valence state-ligand interaction, nature of ligands, and the charge transfer effect. 3d and 4s orbitals of Co, Ni, Cu, and Zn metals are part of the valence state and the distribution of electronic population of the valence band varies according to the central metal atom and ligand interaction. At the same time, this interaction and nature of ligands change the charge transfer between the central atom and ligand. On the other hand, when the conjugation and inductive effect vary according to the changing ligand groups, the charge transfer is affected according to the $-I$ effect. Therefore, these effects can change the K_{β}/K_{α} intensity ratios and ΔE energy differences.

In the present work, the chemical effect on the K_{β}/K_{α} intensity ratios and ΔE energy differences were measured and interpreted without the oxidation number and chemical bond dependence, because we especially chose these complexes which have the same oxidation number and chemical bond between them. Therefore, we tried to interpret chemical effect on the K_{β}/K_{α} intensity ratios and ΔE energy differences in terms of the nature of ligands.

IV. CONCLUSION

The present study demonstrates the existence of chemical effects on Co, Ni, Cu, and Zn complexes. Comparing our experimental K_{β}/K_{α} intensity ratios with available theoretical values and experimental ΔE energy differences with experimental values of pure metals, we found good agreement for the ligand types. Ligand-central metal interaction affects outer shell electrons and this interaction changes the charge transfer between the ligand and central metal atom. Results show that the same ligand type creates almost the same effect on the central metals. To obtain more absolute results about chemical effects on the K_{β}/K_{α} intensity ratios and ΔE energy differences, we plan to extend these measurements for both various elements and var-

ious complexes.

V. ACKNOWLEDGMENT

This work was supported by the Karadeniz Technical University Research Fund (No.2007.111.001.2).

- [1] Ö. Söğüt, S. Seven, E. Baydaş, E. Büyükkasap, and A. Küçükönder, X-Ray Spectrom. **56**, 1367 (2001).
- [2] S. Raj, H. C. Padhi, and M. Polasik, Nucl. Instrum. Methods B **160**, 443 (2000).
- [3] L. Rebohle, U. Lehnert, and G. Zschornack, X-Ray Spectrom. **25**, 295 (1996).
- [4] O. Söğüt, E. Büyükkasap, and H. Erdoğan, Radiat. Phys. Chem. **64**, 343 (2002).
- [5] A. Küçükönder, Y. Şahin, E. Büyükkasap, and A. Kopya, J. Phys. B **26**, 101 (1993).
- [6] G. Brunner, M. Nagel, E. Hartmann, and E. Arndt, J. Phys. B: At. Mol. Phys. **15**, 4517 (1982).
- [7] T. Mukoyama, K. Taniguchi, and H. Adachi, Phys. Rev. B **34**, 3710 (1986).
- [8] F. Folkmann, Nucl. Instrum. Methods B **109/110**, 39 (1996).
- [9] T. Konishi, J. Kawai, M. Fujiwara, T. Kurisaki, H. Wakita, and Y. Gohshi, X-Ray Spectrom. **28**, 470 (1999).
- [10] M. T. Deluigi and J. A. Riveros, Chem. Phys. **325**, 472 (2006).
- [11] R. L. Watson, T. Chiao, and F. E. Jenson, Phys. Rev. Lett. **35**, 254 (1975).
- [12] J. Kawai, M. Ohta, and T. Konishi, Anal. Sci. **21**, 865 (2005).
- [13] M. Y. Apte and C. Mande, J. Phys. C **15**, 607 (1982).
- [14] E. Tıraşoğlu and A. Tekbiyık, Spectrochim. Acta Part B **60**, 549 (2005).
- [15] V. Aylikci, G. Apaydin, E. Tıraşoğlu, N. Kaya, and E. Cengiz, Chem. Phys. **332**, 348 (2007).
- [16] E. Tıraşoğlu, U. Çevik, B. Ertuğral, G. Apaydin, M. Ertuğrul, and A. İ. Kobya, Eur. Phys. J. D **26**, 231 (2003).
- [17] U. Çevik, İ. Değirmencioğlu, B. Ertuğral, G. Apaydin, and H. Baltas, Eur. Phys. J. D **36**, 29 (2005).
- [18] H. Kantekin, A. Bakaray, and Z. Bıyıkhoğlu, Transition Met. Chem. **32**, 209 (2007).
- [19] Z. Bıyıkhoğlu, H. Kantekin, and M. Özil, J. Organomet. Chem. **692**, 2436 (2007).
- [20] H. Kantekin and Z. Bıyıkhoğlu, Dyes and Pigments **77**, 98 (2008).
- [21] Z. Bıyıkhoğlu and H. Kantekin, Transition Met. Chem. **32**, 851 (2007).
- [22] H. Kantekin and Z. Bıyıkhoğlu, Dyes and Pigments **77**, 432 (2008).
- [23] E. Storm and I. H. Israel, Nucl. Data Tables A **7**, 565 (1970).
- [24] J. H. Scofield, Lawrence Livermore Lab. Rep. UCRL-51326, (1973).
- [25] M. O. Krause, J. Phys. Chem. Ref. Data **8**, 307 (1979).
- [26] N. Broll, X-Ray Spectrom. **15**, 271 (1986).
- [27] J. H. Scofield, At. Data Nucl. Data Tables **14**, 121 (1974).
- [28] S. T. Manson and D. J. Kennedy, At. Data Nucl. Data Tables **14**, 111 (1974).